JACS
JOURNAL OF THE AMERICAN CHEMICAL SOCIETY
Article
pubs.acs.org/JACS

Highly Efficient Luminescence of Cu(I) Compounds: Thermally Activated Delayed Fluorescence Combined with Short-Lived Phosphorescence

Thomas Hofbeck,[†] Uwe Monkowius,[‡] and Hartmut Yersin*,[†]

[†]Institut für Physikalische Chemie, Universität Regensburg, D-93053 Regensburg, Germany
[‡]Institute of Inorganic Chemistry, Johannes Kepler University Linz, A-4040 Linz, Austria

Supporting Information

ABSTRACT: Luminescent materials showing thermally activated delayed fluorescence (TADF) have gained high attractiveness as emitters in organic light emitting diodes (OLEDs) and other photonic applications. Nevertheless, even utilization of TADF can be further improved, introducing a novel concept. This is demonstrated by a new class of brightly luminescent low-cost Cu(I) compounds, for which the emission stems from both the lowest excited triplet T_1 and singlet S_1 state. At T = 300 K, these materials exhibit quantum yields of more than Φ_{PL} = 90% at short emission decay times. About 80% of the emission intensity stems from the singlet due to TADF, but importantly, an additional 20% is contributed by the lower lying triplet state according to effective spin−orbit coupling (SOC). SOC induces also a relatively large zero-field splitting of the triplet being unusual for Cu(I) complexes. Thus, the overall emission decay time is distinctly reduced. Combined use of both decay paths opens novel photonic applications, in particular, for OLEDs.

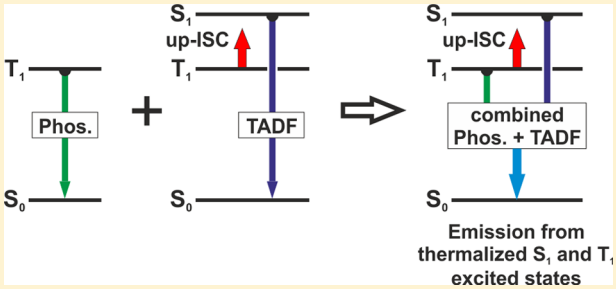

1. INTRODUCTION

In the past decade, phosphorescent metal complexes of the platinum group have been extensively investigated. This research was motivated by a number of applications, especially for organic light emitting diodes (OLEDs).[1,2] Because of high spin−orbit coupling (SOC) induced by the metal centers, these compounds frequently exhibit fast intersystem crossings (ISC) and high radiative triplet decay rates combined with high emission quantum yields. If applied in OLEDs, these complexes can exploit both the singlet and triplet excitons and, principally, can transfer them into light with 100% internal quantum yield,[3,4] representing the triplet harvesting effect.[1−13] Nevertheless, the high costs, unclear toxicities, and problems with respect to blue-light emission of these complexes may be disadvantageous, and therefore, other and more abundant emitter materials are required, for example, compounds based on first-row transition metals. However, the triplet emission (phosphorescence) decay times of these latter materials are normally too long due to the relatively small effectivity of SOC. Thus, application in OLEDs would, for example, result in undesired saturation effects. However, selected Cu(I) compounds may overcome this severe restriction and therefore, have gained increasing attractiveness.[13−33] This is due to the extensive metal-to-ligand charge transfer (MLCT) character of the lowest excited states found for many Cu(I) complexes. The corresponding transitions induce distinct spatial separations of the involved orbitals, in particular of HOMO and LUMO, leading to relatively small exchange integrals and consequently to small energy gaps $\Delta E(S_1 - T_1)$ between the lowest triplet states T_1 and the lowest excited singlet states S_1 (e.g., < 1000 cm^{-1} or 0.12 eV). As a consequence, these materials can show a very efficient thermally activated delayed fluorescence (TADF).[13−17,22,24−26,28−33] Moreover, in Cu(I) complexes, processes of ISC are of the order of 10 ps[34] and therefore, result in a fast thermal equilibration between the T_1 and S_1 states. A prompt fluorescence was not observed. Accordingly, a Boltzmann distribution governs the population ratio of the involved states. Thus, at sufficiently high temperature, the decay of the excited singlet state S_1 to the electronic ground state S_0 dominates the emission decay time, if the corresponding oscillator strength is high enough. In this situation, the decay time at ambient temperature can become orders of magnitude shorter than the triplet decay time. If so, the emission represents a TADF.[13,15−17,29−33,35,36] Indeed, efficient OLEDs with Cu(I) compounds and even organic molecules as emitters have already been realized using this molecular-based TADF mechanism[15,25,28,31,33,37,38] and it could be shown that harvesting of singlet and triplet excitons is successful, though not in the triplet state, but in the thermally activated singlet state. Hence, this mechanism is called "singlet harvesting mechanism".[13,16,17,23,24,28−30,32,33,39]

For many applications, the (radiative) TADF decay time should be as short as possible to overcome saturation effects.

Received: October 29, 2014
Published: December 8, 2014

DOI: 10.1021/ja5109672
J. Am. Chem. Soc. 2015, 137, 399−404

This decay time is strongly governed by the activation energy $\Delta E(S_1 - T_1)$, which should be as small as possible. On the other hand, a small $\Delta E(S_1 - T_1)$ value is usually related to a small oscillator strength of the $S_1 \rightarrow S_0$ fluorescent transition and thus, leads to an undesired relatively long singlet state decay time. This is due to the distinct charge-transfer (CT) character required for obtaining small $\Delta E(S_1 - T_1)$ values. The CT character leads to a small spatial overlap of the wave functions of the excited singlet state S_1 and the ground state S_0 and hence, to a small transition dipole moment. Therefore, an improvement of TADF properties with respect to an increase of the radiative rate is a difficult optimization problem and is faced with limits. Hence, the shortest (radiative) TADF decay times hitherto known, lie in the range of the order of ten μs and thus, do not yet reach the values found for Ir(III) complexes. For example, the well-known $Ir(ppy)_3$ triplet emitter exhibits a (radiative) decay time of about τ = 1.5 to 2 μs.[40−42]

Obviously, alternative strategies for the development of new Cu(I)-based emitters are required. A promising approach is proposed here. An overall faster radiative decay can principally be obtained by opening an *additional* radiative decay path from an additional state, in particular, from the lowest triplet state. But for most Cu(I) complexes known, this $T_1 \rightarrow S_0$ path is largely ineffective due to very weak spin−orbit couplings (SOC) of the T_1 state to higher lying singlet states. As a consequence, the phosphorescence decay time is of the order of several hundred μs and even up to ms.[13−17,22,23,28,32,43] On the other hand, development of complexes that exhibit high SOC efficiency is not unrealistic as is discussed in this study. Here, we present a new class of brightly luminescent dinuclear Cu(I) compounds showing efficient TADF from the S_1 state and direct phosphorescence from the T_1 state both being in a thermal equilibrium. The phosphorescence contributes significantly to the emission due to efficient SOC that induces a relatively short radiative T_1 decay time.

2. THERMALLY ACTIVATED DELAYED FLUORESCENCE

The chemical structures of the new Cu(I) compounds are displayed in Figure 1. The $Cu_2X_2(N\text{^}P)_2$ complexes consist of two Cu(I) ions with (N^P) = 2-(diphenylphosphino)-6-methylpyridine and halide (X = Cl (**1**), Br (**2**), I (**3**)) ligands.

The photophysical investigations carried out in this study reveal a number of previously unknown properties of copper compounds. The materials were analyzed using powder samples. It is remarked that usually solid state samples are not well appropriate for detailed investigations of decay properties because processes, such as triplet−triplet annihilation or energy transfer, can strongly influence deactivation mechanisms. However, for Cu(I) complexes that exhibit low-lying ^{1,3}MLCT states, these effects are not important due to self-trapping mechanisms. They induce a localization of the excitation (self-trapping) and thus, the emission displays largely isolated molecular properties even of the compounds embedded in a crystalline cage of the neat material.[13,16]

The three complexes **1**, **2**, and **3** show intense luminescence under excitation with UV light. The emission of all compounds occurs in the blue-green spectral range with the emission maxima between 485 and 501 nm and emission decay times between 7.3 and 12.4 μs at ambient temperature. The observed emission quantum yields of the presented Cu(I) compounds are close to unity at 77 K and over 50% at ambient temperature, in particular, amounting to Φ_{PL} = 92% for $Cu_2Cl_2(N\text{^}P)_2$ (**1**) at

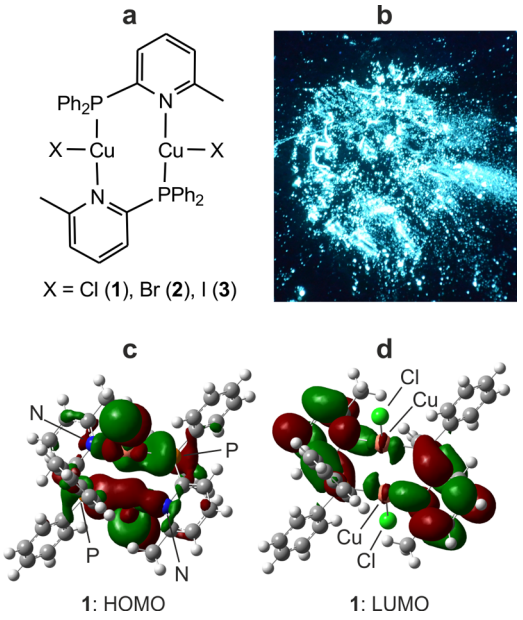

Figure 1. Chemical structure of $Cu_2X_2(N\text{^}P)_2$, photoluminescence, and frontier orbitals of $Cu_2Cl_2(N\text{^}P)_2$ (**1**). (a) Chemical structural formula of $Cu_2X_2(N\text{^}P)_2$. (b) Brightly blue-white emitting powder of $Cu_2Cl_2(N\text{^}P)_2$ (**1**) under UV excitation. (c,d) Frontier orbitals HOMO and LUMO of $Cu_2Cl_2(N\text{^}P)_2$ (**1**) according to a DFT calculation (compare section 5).

300 K. The emission spectra of compound **1**, for example, are shown in Figure 2. The corresponding transitions are assigned to be of ^{1,3}MLCT character as is supported by DFT calculations (Figure 1c,d). Consistently, the spectra are broad and could not be resolved even at T = 1.3 K. At this temperature, the emission maximum lies at 510 nm and is found at almost the same wavelength up to about T = 120 K. However, with further temperature increase to T = 300 K, a blue shift of the maximum by 25 nm (1000 cm^{-1}, 0.12 eV) is observed. In this temperature range, the emission decay time decreases from τ(77 K) = 44 μs to τ(300 K) = 8.3 μs, while the radiative rates increase by a

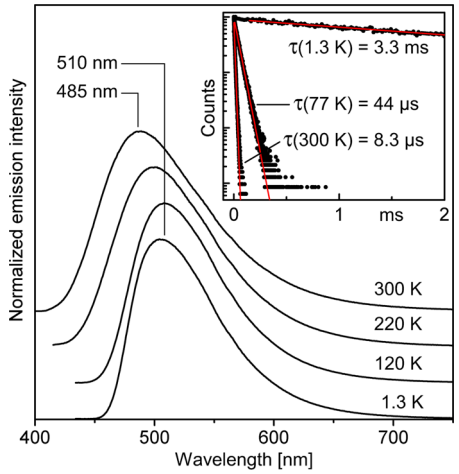

Figure 2. Emission spectra of $Cu_2Cl_2(N\text{^}P)_2$ (compound **1**) at different temperatures. The inset shows the decay behavior at T = 1.3K, 77 K, and 300 K. The decay is monoexponential with decay times of τ(1.3 K) = 3.3 ms, τ(77 K) = 44 μs, and τ(300 K) = 8.3 μs, respectively. Further decay curves measured at different temperatures are given in the Supporting Information (Figure S3).

DOI: 10.1021/ja5109672
J. Am. Chem. Soc. 2015, 137, 399−404

factor of about five from 2.2×10^4 s^{-1} to 11×10^4 s^{-1}. (Table 1) This behavior shows that an emission from a higher lying state being populated at ambient temperature is activated and that this transition carries a significantly larger allowedness than the low-temperature phosphorescence. Combined with the observed blue shift of the spectra upon temperature increase, an occurrence of a TADF is indicated. Similar properties have already been observed and rationalized equivalently for other Cu(I) complexes.[13,15−17,23,24,27−33,35,36] Further support for this assignment will be presented below. The compounds **2** and **3** display an analogous behavior. Photophysical data of the three compounds at ambient temperature and 77 K are summarized in Table 1.

Table 1. Photophysical Data of Powder Samples of $Cu_2X_2(N^P)_2$

X	Cl (**1**)	Br (**2**)	I (**3**)
λ_{max}(300 K) [nm]	485	501	484
Φ_{PL}(300 K) [%][a]	92	52	76
τ(300 K) [μs][b]	8.3	12.4[c]	7.3[c]
k^r(300 K) [s^{-1}][d]	11×10^4	4.2×10^4	10×10^4
k^{nr}(300 K) [s^{-1}]	1.0×10^4	3.9×10^4	3.3×10^4
λ_{max}(77 K) [nm]	510	526	511
Φ_{PL}(77 K) [%][a]	97	97	90
τ(77 K) [μs][b]	44	84[c]	51[c]
k^r(77 K) [s^{-1}][d]	2.2×10^4	1.2×10^4	1.8×10^4
k^{nr}(77 K) [s^{-1}][e]	7×10^2	4×10^2	20×10^2
$\Delta E(S_1 - T_1)$ [cm^{-1}][f]	1000	950	1100

[a]Excitation wavelength λ_{exc} = 400 nm, accuracy of Φ_{PL} at 77 K: ± 10% (rel. err.) and at 300 K: ± 5% (rel. err.). [b]Excitation wavelength λ_{exc} = 372 nm. [c]The decay behavior is not strictly monoexponential; the given value is an intensity weighted average from a biexponential fit. [d]Radiative decay rate $k^r = \Phi_{PL}/\tau$. [e]Nonradiative decay rate $k^{nr} = \tau^{-1} - k^r$. [f]Determined from the emission spectra at 77 K and ambient temperature, respectively (compare also section 3 for a determination of the activation energy).

3. SINGLET AND TRIPLET STATE EMISSION MECHANISMS AND SPIN−ORBIT COUPLING

Subsequently, we want to focus on compound **1** as representative example and investigate the emission decay time over the extended temperature range of 1.3 K ≤ T ≤ 300 K. (Figure 3) The decay is monoexponential in the whole range. At T = 1.3 K, the emission decays with an astonishingly long time of τ = 3.3 ms. With increasing temperature, the decay time shortens drastically within several Kelvin and reaches a plateau near T = 50 K with a decay time of about 44 μs and then drops to ≈8 μs at ambient temperature. As the emission quantum yield is almost constant over the entire temperature range above $T \approx 4$ K (Figure 3), the decrease of the decay time is assigned to be induced by a successive population of different energy states. In particular, in the low-temperature range below T = 20 K, properties of the zero-field split triplet T_1 state are displayed and at higher temperature, above $T \approx 150$ K, the thermal activation of the short-lived singlet state S_1, giving the TADF, is evidenced. For completeness it is remarked that below $T \approx 4$ K, the emission decay time increases from about 200 μs to 3.3 ms. This is related to a strong decrease of the radiative allowedness of the emitting state, representing the lowest triplet substate (see below). Consequently, nonradiative processes become competitive at very low temperature and a slight decrease of the quantum yield results. (Compare[42,44,45])

In a situation of a fast thermalization between the excited states (fast relative to the emission decay times), the overall decay behavior $\tau(T)$ can be described by (in analogy to refs 46−48)

$$\tau(T) = \frac{1 + \exp\left(-\frac{\Delta E(\mathrm{II}-\mathrm{I})}{k_B T}\right) + \exp\left(-\frac{\Delta E(\mathrm{III}-\mathrm{I})}{k_B T}\right) + \exp\left(-\frac{\Delta E(S_1-\mathrm{I})}{k_B T}\right)}{\frac{1}{\tau(\mathrm{I})} + \frac{1}{\tau(\mathrm{II})}\exp\left(-\frac{\Delta E(\mathrm{II}-\mathrm{I})}{k_B T}\right) + \frac{1}{\tau(\mathrm{III})}\exp\left(-\frac{\Delta E(\mathrm{III}-\mathrm{I})}{k_B T}\right) + \frac{1}{\tau(S_1)}\exp\left(-\frac{\Delta E(S_1-\mathrm{I})}{k_B T}\right)} \quad (1)$$

with I, II, III representing the T_1 substates and S_1 the singlet state, respectively. Fitting of eq 1 to the experimental data of the emission decay times (Figure 3) leads to a well matching fit curve and reveals the individual emission decay times and energy separations of the involved states (Figure 4). The splittings of the triplet substates amount to $\Delta E(\mathrm{II} - \mathrm{I}) = 7$ cm^{-1} and $\Delta E(\mathrm{III} - \mathrm{I}) = \Delta E(\mathrm{ZFS}) = 15$ cm^{-1} with emission decay times of the substates of τ_I = 3.5 ms, τ_{II} = 30 μs, and τ_{III} = 26 μs. Such large splittings have not been observed so far for copper compounds. The TADF is characterized by an activation energy of $\Delta E(S_1 - \mathrm{I}) \approx \Delta E(S_1 - T_1) = 930$ cm^{-1} and a spontaneous decay time of the S_1 state of $\tau(S_1)$ = 40 ns. The S_1 decay was not observed directly, obviously, the ISC time is much faster than 40 ns. Therefore, the fast ISC leads to a fast population of the triplet state T_1 and the prompt fluorescence is quenched. The time constant of 40 ns or more exactly the related radiative decay rate represents the probability of the transition between the excited singlet state S_1 and the electronic ground state S_0. The activation energy resulting from the fit corresponds well to the energy separation between the emission maxima at T = 77 and 300 K. (Figure 2)

Importantly, the results show that at ambient temperature the emission properties of $Cu_2Cl_2(N^P)_2$ (**1**) are determined by *both* the lowest excited T_1 and S_1 states. Roughly 80% of the emission intensity stems from the S_1 state as TADF, while the

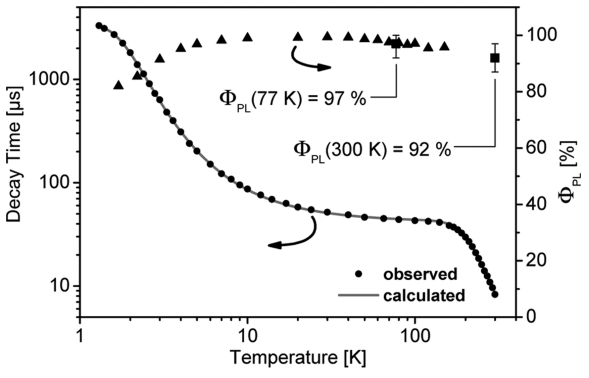

Figure 3. Temperature dependence of the emission decay time and the quantum yield of $Cu_2Cl_2(N^P)_2$ (compound **1**). The decay behavior was monoexponential in the investigated temperature range. The calculated fit function is based on eq 1, see text.

DOI: 10.1021/ja5109672
J. Am. Chem. Soc. 2015, 137, 399−404

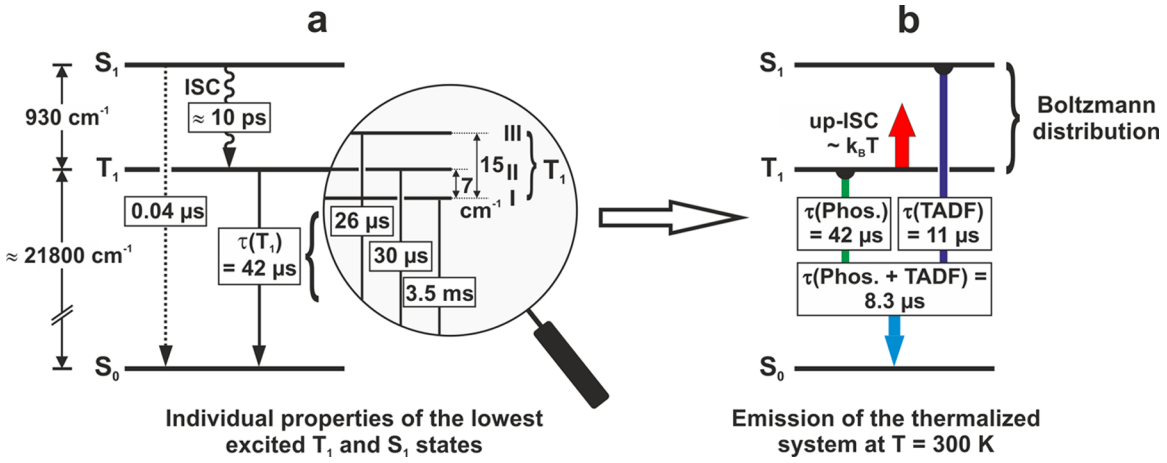

Figure 4. Energy level scheme for $Cu_2Cl_2(N^P)_2$ (**1**). (a) The energy separations of the excited states and time constants of the transitions between the excited states and the ground state result from a fit procedure by use of eq 1. $\tau(T_1)$ = 42 μs represents the average decay time of the three sublevels of the triplet state T_1. ISC and up-ISC represent the intersystem crossing (in several ps)[34] and the thermally activated up-intersystem crossing (= reverse ISC) processes, respectively. Because of the fast ISC in the order of 10 ps no prompt fluorescence $S_1 \rightarrow S_0$ has been observed. The time constant of 40 ns corresponds to the probability of the $S_1 \leftrightarrow S_0$ transition. For completeness, it is remarked that use of a four excited state model is required due to the high effectivity of SOC in compound **1**, resulting in a remarkable zero-field splitting of the triplet state T_1 of 15 cm^{-1} and in short emission decay times of the triplet substates II and III. (b) At a temperature of T = 300 K, the emission stems from the triplet T_1 (as phosphorescence) *and* from the singlet S_1 due to TADF. The overall emission decay time amounts to τ(300 K) = 8.3 μs, whereas the TADF path contributes with a decay time constant of 11 μs and the phosphorescence decay path with a time constant of 42 μs.

remaining 20% are contributed by the energetically lower lying triplet state. (Figure 5a and Supporting Information) This is

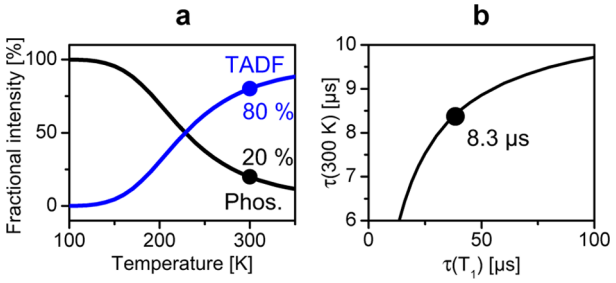

Figure 5. Simulation of the fractional emission intensities and emission decay times. (a) Fractional emission intensities (simulation results) stemming from TADF and direct phosphorescence in dependence of temperature, respectively, calculated on the basis of the experimental data from Figure 4. The points characterize the properties of compound **1** at ambient temperature. (b) Simulation results of the overall emission decay time τ(300 K) (TADF + phosphorescence) versus the decay time of the triplet state $\tau(T_1)$. The TADF-only decay time (for T = 300 K and $\tau(T_1) > 1000$ μs) amounts to about 11 μs. With an additional decay channel via the triplet state with a decay time of $\tau(T_1)$ = 42 μs the overall decay time is reduced to 8.3 μs (experimental point). (Simulation background is provided in the Supporting Information).

due to the relatively high $T_1 \rightarrow S_0$ rate of $k(T_1) = 2.4 \times 10^4$ s^{-1} or the corresponding short decay time of $\tau(T_1)$ = 42 μs. This value is calculated as an average from the individual decay times of the three T_1 substates according to eq S7 (see Supporting Information). It is remarked that this calculated time constant deviates only slightly from the experimentally measured value of τ(77 K) = 44 μs (compare Table 1), thus, supporting the presented model. (Figure 4) The relatively large rate of the $T_1 \rightarrow S_0$ transition is a result of a significant efficiency of SOC, which is distinctly more effective for the investigated complexes than for other Cu(I) complexes hitherto studied.[13,15−17,23,32,43,48] Accordingly, the additional radiative decay path from the T_1 state leads to a distinct reduction of the overall emission decay time by about 20% as compared to a TADF-only process in the assumed case of a very long T_1 decay. (Figure 5b)

SOC is also responsible for the large zero-field splitting of T_1 of ΔE(ZFS) = 15 cm^{-1}, representing the largest value found for ^{3}MLCT states of Cu(I) complexes up to now. (Figure 4a) An explanation for the high SOC efficiency in the present compound can be traced back to the energy separations between the populated d-orbitals in the HOMO range. As discussed in detail by Yersin et al.,[13,49,50] SOC between MLCT states is effective between energy states that result from *different* d-orbital character. For example, an emitting T_1 state of $^3d_1\pi^*$ character can experience significant SOC by mixing with $^{1,3}d_2\pi^*$ states but not with a state of the same configuration, i.e., not with the $^1d_1\pi^*$ state. Such quantum mechanical mixings provide radiative rates to the $T_1 \leftrightarrow S_0$ transition and lead to a large ZFS of the lowest $^3d\pi^*$ (^{3}MLCT) state. Moreover, since the strengths of state mixings are usually determined by energy separations between these states according to perturbation theory approaches and since the energies of the corresponding states are very roughly given by the energies of the occupied frontier orbitals of different d-orbital character (such as HOMO, HOMO−1, ...), simple DFT calculations may allow us to elucidate trends of the SOC efficiencies for different Cu(I) complexes. Interestingly, a comparison between two Cu(I) dimers, compound **1** and $[Cu(\mu\text{-}Cl)(PNMe_2)]_2$ (compound **4**) with $PNMe_2$ = Ph_2P-(*o*-C_6H_4)-$N(CH_3)_2$,[23] displays the discussed differences of the T_1 state properties clearly. In particular, the radiative rates and zero-field splittings of compound **4** are small with $k^r(T_1) = 0.4 \times 10^4$ s^{-1} and ΔE(ZFS) < 1 to 2 cm^{-1}, respectively,[23] while the corresponding values for compound **1** are significantly larger amounting to $k(T_1) = 2.4 \times 10^4$ s^{-1} and ΔE(ZFS) = 15 cm^{-1}. Indeed, this trend is related to the d-orbital splittings (represented by the energy separations of HOMO and

DOI: 10.1021/ja5109672
J. Am. Chem. Soc. 2015, 137, 399−404

HOMO−1 with different d-orbital character according to DFT calculations) amounting to ≈1 eV for **4** but only to ≈0.3 eV for **1**. Obviously, the structure of compound **1** favors a small d-orbital splitting and thus, opens the strong direct phosphorescent radiative path.

4. CONCLUSION

A detailed photophysical study of a series of new Cu(I) dimers of a $Cu_2X_2(N^P)_2$ structure (X = Cl (**1**), Br (**2**), I (**3**)) reveals insight into the emission behavior. In particular, the materials are efficient TADF emitters giving relatively short TADF decay times at ambient temperature and thus, represent good candidates for OLED applications. Furthermore, focusing on the bright $Cu_2Cl_2(N^P)_2$ emitter (Φ_{PL} = 92%), it is shown that in this case, copper can also provide significant SOC resulting in an efficient phosphorescence path in addition to the TADF path. This is evidenced by the relatively high $T_1 \rightarrow S_0$ rate of $k(T_1) = 2.4 \times 10^4\ s^{-1}$ and the large zero-field splitting of the T_1 of $\Delta E(ZFS) = 15\ cm^{-1}$. Accordingly, the emission at ambient temperature consists of two decay paths, i.e., of 20% direct phosphorescence and 80% TADF-only contribution. Interestingly, the size of $\Delta E(ZFS)$ of $Cu_2Cl_2(N^P)_2$ (**1**) is in the order of that of typical platinum compounds with significant MLCT (metal-to-ligand charge transfer) contribution (compare[13,48−52]). This is rather unexpected for the light metal ion Cu(I). The additional phosphorescence path opened by efficient SOC reduces the overall emission decay time by about 20% as compared to the TADF-only emission. Obviously, the combined use of two decay paths represents a very promising new strategy for engineering novel and better low-cost OLED emitter materials.

5. EXPERIMENTAL SECTION

Synthesis. The respective copper(I) halide (0.36 mmol: CuCl 24 mg, CuBr 52 mg, CuI 69 mg) and diphenylphosphanyl-6-methylpyridine (0.36 mmol, 100 mg) are stirred in a 1:1 molar ratio in dichloromethane (10 mL) under ambient conditions overnight. The product is precipitated by addition of diethyl ether as yellow, microcrystalline powder. Crystals suitable for X-ray diffraction are obtained by slow gas phase diffusion of diethyl ether into the filtered reaction mixture. Once the solid complexes are formed, they are only slightly soluble thus hampering NMR spectroscopy. Yield (%): Cl 76%; Br 81%; I 83%. Elemental analysis calcd (%) for $C_{36}H_{32}N_2P_2Cu_2Cl_2$: C 57.45, H 4.29, N 3.72; found: C 57.44, H 4.30, N 3.63; calcd (%) for $C_{36}H_{32}N_2P_2Cu_2Br_2$: C 51.38, H 3.83, N 3.33; found: C 50.98, H 3.86, N 3.08; calcd (%) for $C_{36}H_{32}N_2P_2Cu_2I_2$: C 46.22, H 3.45, N 2.99; found: C 46.12, H 3.48, N 3.11. Further information about the synthesis and the crystal structures are provided in the Supporting Information.

Photophysical Characterization. The copper compounds were investigated as powder. Emission spectra and decay curves were measured by use of a Fluorolog 3 spectrometer (Horiba Jobin Yvon) equipped with a cooled photomultiplier tube. The spectra were corrected with respect to the wavelength dependence of the spectrometer/detector. The decay behavior of the phosphorescence was recorded using a multichannel scaler card (P7887, Fast ComTec) with a time resolution of 250 ps. For excitation, a pulsed diode laser (378 nm, pulse width <70 ps, PicoBrite, Horiba) was used. A cryostat Konti IT (CryoVac) was applied for the variation of temperature between 1.3 and 300 K. Quantum yield measurements at ambient temperature and at 77 K were carried out with an integrating sphere applying a C9920−02 system (Hamamatsu). For quantum yields at other temperatures, the integrated emission intensity, being proportional to the photoluminescence quantum yield Φ_{PL}, was measured. Subsequently, these relative quantum yield data were calibrated by use of the absolute Φ_{PL} values measured at 300 and 77 K. All samples were measured under inert gas (He, N_2).

DFT Calculations. The frontier orbitals (HOMO, LUMO) and the energy separations of HOMO and HOMO−1 were obtained by DFT calculations with the Gaussian 09 software[53] using the B3LYP functional and the m6-31G*[54] basis set for Cu and the 6-311G* basis set for all other atoms. The calculations were performed in the T_1 optimized geometry.

■ ASSOCIATED CONTENT

Supporting Information

Synthesis and crystal structures. Decay behavior of $Cu_2Cl_2(N^P)_2$. Equations for fractional emission intensities and emission decay time at ambient temperature. This material is available free of charge via the Internet at http://pubs.acs.org.

■ AUTHOR INFORMATION

Corresponding Author

hartmut.yersin@ur.de

Notes

The authors declare no competing financial interest.

■ ACKNOWLEDGMENTS

The BMBF (German Federal Ministry of Education and Research) is acknowledged for the funding of our research. The authors thank Dr. Manfred Zabel for stimulating discussions with respect to the crystallographic analysis.

■ REFERENCES

(1) Yersin, H., Ed.; *Highly Efficient OLEDs with Phosphorescent Materials*; Wiley-VCH: Weinheim, 2008.
(2) Brütting, W., Adachi, C., Eds.; *Physics of Organic Semiconductors*; Wiley-VCH: Weinheim, 2012.
(3) Adachi, C.; Baldo, M. A.; Thompson, M. E.; Forrest, S. R. *J. Appl. Phys.* **2001**, *90*, 5048−5051.
(4) Yersin, H. *Top. Curr. Chem.* **2004**, *241*, 1−26.
(5) Baldo, M. A.; O'Brien, D. F.; You, Y.; Shoustikov, A.; Sibley, S.; Thompson, M. E.; Forrest, S. R. *Nature* **1998**, *395*, 151−154.
(6) Baldo, M. A.; Lamansky, S.; Burrows, P. E.; Thompson, M. E.; Forrest, S. R. *Appl. Phys. Lett.* **1999**, *75*, 4−6.
(7) Adachi, C.; Baldo, M. A.; Forrest, S. R.; Thompson, M. E. *Appl. Phys. Lett.* **2000**, *77*, 904−906.
(8) Xiao, L.; Chen, Z.; Qu, B.; Luo, J.; Kong, S.; Gong, Q.; Kido, J. *Adv. Mater.* **2011**, *23*, 926−952.
(9) Kalinowski, J.; Fattori, V.; Cocchi, M.; Williams, J. A. G. *Coord. Chem. Rev.* **2011**, *255*, 2401−2425.
(10) Che, C.-M.; Kwok, C.-C.; Lai, S.-W.; Rausch, A. F.; Finkenzeller, W. J.; Zhu, N.; Yersin, H. *Chem.—Eur. J.* **2010**, *16*, 233−247.
(11) Chi, Y.; Chou, P.-T. *Chem. Soc. Rev.* **2010**, *39*, 638−655.
(12) Borek, C.; Hanson, K.; Djurovich, P.; Thompson, M.; Aznavour, K.; Bau, R.; Sun, Y.; Forrest, S.; Brooks, J.; Michalski, L.; Brown, J. *Angew. Chem., Int. Ed.* **2007**, *46*, 1109−1112.
(13) Yersin, H.; Rausch, A. F.; Czerwieniec, R.; Hofbeck, T.; Fischer, T. *Coord. Chem. Rev.* **2011**, *255*, 2622−2652.
(14) Tsuboyama, A.; Kuge, K.; Furugori, M.; Okada, S.; Hoshino, M.; Ueno, K. *Inorg. Chem.* **2007**, *46*, 1992−2001.
(15) Deaton, J. C.; Switalski, S. C.; Kondakov, D. Y.; Young, R. H.; Pawlik, T. D.; Giesen, D. J.; Harkins, S. B.; Miller, A. J. M.; Mickenberg, S. F.; Peters, J. C. *J. Am. Chem. Soc.* **2010**, *132*, 9499−9508.
(16) Czerwieniec, R.; Yu, J.; Yersin, H. *Inorg. Chem.* **2011**, *50*, 8293−8301.
(17) Czerwieniec, R.; Kowalski, K.; Yersin, H. *Dalton Trans.* **2013**, *42*, 9826−9830.
(18) Wada, A.; Zhang, Q.; Yasuda, T.; Takasu, I.; Enomoto, S.; Adachi, C. *Chem. Commun.* **2012**, *48*, 5340−5342.

DOI: 10.1021/ja5109672
J. Am. Chem. Soc. 2015, 137, 399−404

(19) Lotito, K. J.; Peters, J. C. *Chem. Commun.* **2010**, *46*, 3690−3692.
(20) Krylova, V. A.; Djurovich, P. I.; Whited, M. T.; Thompson, M. E. *Chem. Commun.* **2010**, *46*, 6696−6698.
(21) Liu, Z.; Qayyum, M. F.; Wu, C.; Whited, M. T.; Djurovich, P. I.; Hodgson, K. O.; Hedman, B.; Solomon, E. I.; Thompson, M. E. *J. Am. Chem. Soc.* **2011**, *133*, 3700−3703.
(22) Osawa, M. *Chem. Commun.* **2014**, *50*, 1801−1803.
(23) Leitl, M. J.; Küchle, F.-R.; Mayer, H. A.; Wesemann, L.; Yersin, H. *J. Phys. Chem. A* **2013**, *117*, 11823−11836.
(24) Zink, D. M.; Bächle, M.; Baumann, T.; Nieger, M.; Kühn, M.; Wang, C.; Klopper, W.; Monkowius, U.; Hofbeck, T.; Yersin, H.; Bräse, S. *Inorg. Chem.* **2013**, *52*, 2292−2305.
(25) Igawa, S.; Hashimoto, M.; Kawata, I.; Yashima, M.; Hoshino, M.; Osawa, M. *J. Mater. Chem. C* **2013**, *1*, 542−551.
(26) Zink, D. M.; Grab, T.; Baumann, T.; Nieger, M.; Barnes, E. C.; Klopper, W.; Bräse, S. *Organometallics* **2011**, *30*, 3275−3283.
(27) Wallesch, M.; Volz, D.; Zink, D. M.; Schepers, U.; Nieger, M.; Baumann, T.; Bräse, S. *Chem.—Eur. J.* **2014**, *20*, 6578−6590.
(28) Chen, X.-L.; Yu, R.; Zhang, Q.-K.; Zhou, L.-J.; Wu, X.-Y.; Zhang, Q.; Lu, C.-Z. *Chem. Mater.* **2013**, *25*, 3910−3920.
(29) Leitl, M. J.; Krylova, V. A.; Djurovich, P. I.; Thompson, M. E.; Yersin, H. *J. Am. Chem. Soc.* **2014**, *136*, 16032−16038.
(30) Gneuß, T.; Leitl, M. J.; Finger, L. H.; Rau, N.; Yersin, H.; Sundermeyer, J. *Dalton Trans.* **2015**, DOI: 10.1039/C4DT02631D.
(31) Osawa, M.; Hoshino, M.; Hashimoto, M.; Kawata, I.; Igawa, S.; Yashima, M. *Dalton Trans.* **2015**, DOI: 10.1039/C4DT02853H.
(32) Yersin, H.; Leitl, M. J.; Czerwieniec, R. *Proc. SPIE* **2014**, *9183*, 91830N-1.
(33) Wallesch, M.; Volz, D.; Fléchon, C.; Zink, D. M.; Bräse, S.; Baumann, T. *Proc. SPIE* **2014**, *9183*, 918309-1.
(34) Iwamura, M.; Watanabe, H.; Ishii, K.; Takeuchi, S.; Tahara, T. *J. Am. Chem. Soc.* **2011**, *133*, 7728−7736.
(35) Blasse, G.; McMillin, D. R. *Chem. Phys. Lett.* **1980**, *70*, 1−3.
(36) Kirchhoff, J. R.; Gamache, R. E.; Blaskie, M. W.; Del Paggio, A. A.; Lengel, R. K.; McMillin, D. R. *Inorg. Chem.* **1983**, *22*, 2380−2384.
(37) Uoyama, H.; Goushi, K.; Shizu, K.; Nomura, H.; Adachi, C. *Nature* **2012**, *492*, 234−238.
(38) Zhang, Q.; Li, B.; Huang, S.; Nomura, H.; Tanaka, H.; Adachi, C. *Nat. Photonics* **2014**, *8*, 326−332.
(39) Yersin, H.; Monkowius, U. Singlet Harvesting Effect. International Patents WO 2010/006681 A1 and DE 10 2008 033 563 A1, 2008.
(40) King, K. A.; Spellane, P. J.; Watts, R. J. *J. Am. Chem. Soc.* **1985**, *107*, 1431−1432.
(41) Dedeian, K.; Djurovich, P. I.; Garces, F. O.; Carlson, G.; Watts, R. J. *Inorg. Chem.* **1991**, *30*, 1685−1687.
(42) Hofbeck, T.; Yersin, H. *Inorg. Chem.* **2010**, *49*, 9290−9299.
(43) Smith, C. S.; Mann, K. R. *J. Am. Chem. Soc.* **2012**, *134*, 8786−8789.
(44) Hager, G. D.; Crosby, G. A. *J. Am. Chem. Soc.* **1975**, *97*, 7031−7037.
(45) Hager, G. D.; Watts, R. J.; Crosby, G. A. *J. Am. Chem. Soc.* **1975**, *97*, 7037−7042.
(46) Striplin, D. R.; Crosby, G. A. *Chem. Phys. Lett.* **1994**, *221*, 426−430.
(47) Azumi, T.; Miki, H. *Top. Curr. Chem.* **1997**, *191*, 1−40.
(48) Yersin, H.; Rausch, A. F.; Czerwieniec, R. In *Physics of Organic Semiconductors*; Brütting, W., Adachi, C., Eds.; Wiley-VCH: Weinheim, 2012; pp 371−424.
(49) Yersin, H.; Finkenzeller, W. J. In *Highly Efficient OLEDs with Phosphorescent Materials*; Yersin, H., Ed.; Wiley-VCH: Weinheim, 2008; pp 1−97.
(50) Rausch, A. F.; Homeier, H. H. H.; Yersin, H. *Top. Organomet. Chem.* **2010**, *29*, 193−235.
(51) Wiedenhofer, H.; Schützenmeier, S.; von Zelewsky, A.; Yersin, H. *J. Phys. Chem.* **1995**, *99*, 13385−13391.
(52) Rausch, A. F.; Murphy, L.; Williams, J. A. G.; Yersin, H. *Inorg. Chem.* **2009**, *48*, 11407−11414.
(53) Frisch, M. J.; Trucks, G. W.; Schlegel, H. B.; Scuseria, G. E.; Robb, M. A.; Cheeseman, J. R.; Scalmani, G.; Barone, V.; Mennucci, B.; Petersson, G. A.; Nakatsuji, H.; Caricato, M.; Li, X.; Hratchian, H. P.; Izmaylov, A. F.; Bloino, J.; Zheng, G.; Sonnenberg, J. L.; Hada, M.; Ehara, M.; Toyota, K.; Fukuda, R.; Hasegawa, J.; Ishida, M.; Nakajima, T.; Honda, Y.; Kitao, O.; Nakai, H.; Vreven, T.; Montgomery, J. A., Jr.; Peralta, J. E.; Ogliaro, F.; Bearpark, M.; Heyd, J. J.; Brothers, E.; Kudin, K. N.; Staroverov, V. N.; Keith, T.; Kobayashi, R.; Normand, J.; Raghavachari, K.; Rendell, A.; Burant, J. C.; Iyengar, S. S.; Tomasi, J.; Cossi, M.; Rega, N.; Millam, J. M.; Klene, M.; Knox, J. E.; Cross, J. B.; Bakken, V.; Adamo, C.; Jaramillo, J.; Gomperts, R.; Stratmann, R. E.; Yazyev, O.; Austin, A. J.; Cammi, R.; Pomelli, C.; Ochterski, J. W.; Martin, R. L.; Morokuma, K.; Zakrzewski, V. G.; Voth, G. A.; Salvador, P.; Dannenberg, J. J.; Dapprich, S.; Daniels, A. D.; Farkas, O.; Foresman, J. B.; Ortiz, J. V.; Cioslowski, J.; Fox, D. J. *Gaussian 09*, Revision B.01; Gaussian, Inc.: Wallingford, CT, 2010.
(54) Mitin, A. V.; Baker, J.; Pulay, P. *J. Chem. Phys.* **2003**, *118*, 7775−7782.

DOI: 10.1021/ja5109672
J. Am. Chem. Soc. 2015, 137, 399−404